Eur Radiol (2003) 13:1148–1153
DOI 10.1007/s00330-002-1614-9

PHYSICS

Mathias Cohnen
Ludger W. Poll
Claudia Puettmann
Klaus Ewen
Andreas Saleh
Ulrich Mödder

Effective doses in standard protocols for multi-slice CT scanning

Received: 18 March 2002
Revised: 21 June 2002
Accepted: 28 June 2002
Published online: 27 July 2002

M. Cohnen (✉) · L.W. Poll · A. Saleh
U. Mödder
Institute of Diagnostic Radiology,
University Hospital,
Heinrich Heine University, Moorenstrasse 5,
40225 Düsseldorf, Germany
e-mail: cohnen @ med.uni-duesseldorf.de
Tel.: +49-211-8117752
Fax: +49-211-8116145

C. Puettmann · K. Ewen
State Institute for Occupational Safety and
Health of North Rhine-Westfalia,
40225 Düsseldorf, Germany

Abstract The purpose of this study was to assess the radiation exposure of patients in several standard protocols in multi-slice CT (MSCT). Scanning protocols for neck, chest, abdomen, and spine were examined on a Somatom Plus 4 Volume Zoom MSCT (Siemens, Erlangen, Germany) with changing slice collimation (4×1, 4×2.5, and 4×5 mm), and pitch factors (1, 1.5, and 2). Effective doses were calculated from LiF–TLD measurements at several organ sites using an Alderson-Rando phantom and compared with calculations using the weighted CTDI. Effective dose for MSCT of the neck was 2.8 mSv. For different protocols for MSCT of the chest, 7.5–12.9 mSv were found. In abdominal MSCT protocols, effective dose varied between 12.4 and 16.1 mSv. The MSCT of the spine may lead to 12 mSv. An excellent correlation between the effective dose as determined by LiF–TLD and the calculated effective dose using the weighted CTDI could be demonstrated; however, a difference of up to 30% (mean 14.3%) was noted. Standard protocols for MSCT as measured in this study showed effective doses of up to16 mSv. Phantom measurement data show a good correlation to estimations using the weighted CTDI.

Keywords Radiation exposure · Multi-slice CT · Effective dose · Alderson-Rando phantom

Introduction

The introduction of multi-row detector CT or multi-slice CT (MSCT) into clinical routine has increased patient comfort with shorter breath-hold periods and opened new fields to radiological diagnostics [1]. Cardiac CT, large-volume high-resolution CT, and improved z-plane resolution are new goals of CT diagnostics [2, 3, 4, 5]. As CT increases the collective radiation dose given for medical purposes disproportionate to its frequency of utilization, this study was performed to assess radiation dose in different MSCT protocols for standard examinations of the neck, chest, abdomen, and lumbar spine [6]. A further increase in radiation exposure of the patient is to be assumed in an expanding diagnostic work-up [7]. For reference reasons we compared the measured data to calculations of the effective doses using the weighted CTDI given by the implemented software.

Materials and methods

Dose measurements were performed on a multi-row detector CT scanner (MSCT) Somatom Plus 4 Volume Zoom with the standard software Somaris/5 VA 20 A (both from Siemens, Erlangen, Germany). Technical parameters of the different CT examinations are given in Table 1.

The MSCT scanner used in this study allows a slice collimation from 0.5 to 5 mm. For chest CT, a slice collimation was set to 1 (protocol HiRes), 2.5 (protocol Routine), and 5 mm (protocol Fast), and pitch factors of 8, 6, and 6 were chosen; thus, a table feed of 8, 15, or 30 mm per rotation resulted with a tube rotation time of 0.5 s. For MSCT of the abdomen, 1 (protocol Angio), 2.5 (protocol Routine), and 5 mm (protocol Fast) slice collimation was set with a pitch of 8, 6, and 5, respectively. The Neck protocol

Table 1 Parameters of different scan protocols. Pitch (volume) *p'* is the volume–pitch for MSCT (table feed per slice thickness). Pitch *p* corresponds to table feed per total collimation considering the number of detector rows acquiring simultaneously. *Diff. scan length/total feed*: "overscan" area resulting from the difference between the total table feed [table feed×(scan time/rotation time)] and the scan length as planned

	Neck	Chest			Abdomen			Spine
		Fast	Routine	HiRes	Fast	Routine	Angio	
Slice thickness (mm)	1	5	2.5	1	5	2.5	1	2.5
Table feed (mm)	6	30	15	8	25	15	8	10
Pitch (volume) p'	6	6	6	8	5	6	8	4
Pitch p	1.5	1.5	1.5	2	1.25	1.5	2	1
Current (mAs)	100	120	120	70	165	130	100	130
Potential (kV)	120	140	140	140	120	120	120	140
Rotation time (s)	0.5	0.5	0.5	0.5	0.5	0.5	0.5	0.75
Scan length (mm)	225	300	333	298	467	418	429	251
Scan time (s)	19.75	5.68	12.2	19.4	10.1	14.84	27.61	20.66
$CTDI_{w,eff}$ (mGy)	11.4	14.9	16.4	11.6	14.2	12.2	11.4	17.9
Diff. scan length/total feed (mm)	12	40.8	33	12.4	38	27.2	12.76	24.5

consisted of a 1-mm collimation with a Pitch of 8 while the lumbar "Spine" protocol uses a 2.5-mm collimation with a pitch of 4.

Tube current was 120 mAs for chest MSCT with a reduced tube current for the HiRes protocol (70 mAs). For abdominal MSCT protocols, tube current was gradually reduced from 165 (Fast) to 130 (Routine) and 100 mAs (Angio) with decreasing slice collimation (see Table 1). For the Neck protocol, the tube current was set to 100 mAs, and the Spine protocol was performed with 130 mAs, respectively.

After acquisition of a digital projection radiograph (topogram), chest CTs were planned to cover the area from the suprasternal notch to the pulmonary recess, whereas abdomen CTs were planned to reach from the hepatic dome to the perineum. For the Neck protocol, the scan started at the skull base extending to the suprasternal notch. The lumbar spine scan was estimated from L1 to L5. As the Alderson-Rando phantom is built from 34 single slabs of 2.5-cm thickness, the topogram allows an exact planning to include the same number and range of slabs [8]. Due to the manual placement of scan coverage, the scan length in chest and abdominal protocols differ slightly; however, this did not affect the exposure of TLD, as these sites were chosen in a way that TLDs either were definitely exposed by the primary beam or by scatter radiation only.

An Alderson-Rando anthropomorphic phantom was used to assess radiation exposure [8]. Depending on the scan protocol, it was equipped with at least 30 LiF–thermoluminescent dosimeters, which were analyzed using a Glowcurve analyzer Harshaw filtrol 2000D (Harshaw, Cleveland, Ohio). Within 12 h after exposure, TLD were read out so that fading was nearly avoided. In order to transfer the measured electrical charge (nC) into dose values (mGy), data had to be multiplied with a correction factor. This correction factor of 0.82 mGy/nC resulted from calibration measurements taking into account the beam filter of the Volume Zoom of 1.4 mm aluminum and 1.2 mm titanium. As the dose detection threshold of LiF–TLD is relatively high, TLD were read out after all CT-protocols were repeated four times [9]. The resulting data were divided by four.

Positions of TLD were chosen such that all organs within the primary beam were covered. Additionally, radiation-sensitive organs, such as the ovaries and testes, were included. One TLD was positioned per location with at least two TLD forming the basis for organ doses. Data from TLD directly positioned within an organ (thyroid, gonads) were directly used to define the organ dose after addition of the measured values and division by the number of TLD. For larger structures or organs (e.g., lungs, liver, esophagus), the organ dose was defined as mean of at least three TLD positioned in the region of this organ. Organ dose of the red bone marrow was calculated by adding data from TLD in several locations (clavicle, scapula, sternum, two ribs, thoracic and lumbar vertebrae, and pelvis) and multiplying with the relative red marrow distribution in the different bones. The surface dose was derived from a total of three groups of three TLD each positioned on the surface of the phantom. Due to the rotation of the tube, radiation exposure is expected on all sides of the phantom; thus, two TLD packs were positioned on the front and one on the back of the phantom within the area of the primary beam. Although skin dose should be measured 0.7 mm under the surface, a detectable difference in the surface is not to be expected. As it is difficult to define and to reproduce the correct percentage of how much surface or skin might have been exposed, we calculated the effective dose from the data measured in the primary beam taking into account that the effective dose might be lower in reality; however, as the weighting factor for skin is 0.01, the influence will only be marginal.

The total effective dose results from addition of the single-organ doses after multiplication with the weighting factor [10]. Separate calculations for male and female patients were done as different organs and therefore organ doses are relevant [11].

The implemented standard CT software (Somaris/5 VA 20 A, Siemens, Erlangen, Germany) displays the effective weighted CTDI ($CTDI_{w,eff}$) computed from the examination settings. Using this $CTDI_{w,eff}$ we calculated the effective dose according to the following equation:

$$E[\mathrm{mSv}] = CTDI_{w,eff} \times (n \times TF) \times 1/P_B \times f_{mean} \times k_{CT},$$

where $CTDI_{w,eff}$ is effective weighted CTDI (mGy); (n×TF) is scan length (cm); P_B is conversion of $CTDI_{w,eff}$ to $CTDI_{Air}$ (=0.38); f_{mean} is mean of organ conversion factors [mSv/(mGy×cm)]; and k_{CT} is scanner-specific correction factor dependent on kilovoltage [12, 13].

As dose length product is often recommended to be used as the reference dose quantity, this parameter was determined according to the following equation:

$$DLP[\mathrm{mGy} \times \mathrm{cm}] = CTDI_{w,eff} \times n \times N \times h,$$

where $CTDI_{w,eff}$ is effective weighted CTDI (mGy); n is tube rotations; N is number of detectors; and h is slice thickness (in centimeters) [12, 13].

The total table feed was calculated using the scan parameters given in Table 1. It results from the equation: table feed × (scan time/rotation time).

"Overscan" is the difference between this total table feed and the scan length as planned and indicated by the CT software.

Table 2 Organ doses (mGy) measured by LiF–TLD in several positions for different scan protocols

(mGy)	Neck	Chest			Abdomen			Spine
		Fast	Routine	HiRes	Fast	Routine	Angio	
Thyroid	11.6	28.9	23.8	15.4	0	0	0	0
Esophagus	25.7	20.8	27.9	13.3	3.9	1.6	1.5	0
Lung	1.5	23	25.4	17.1	8.3	3.5	3	0
Female breast	0.8	17.5	19.9	6.5	2.7	1.7	1.3	0
Liver	0	19.5	15	11.8	23.5	20.6	19.5	28.1
Stomach	0	25	26	15.8	24.9	20.8	21.4	27.3
Colon	0	1	1.4	0.7	23.6	21.3	20.4	30.4
Gonads (ovaries)	0	0.3	0.4	0.3	20.5	18.2	17.8	8.7
Gonads (testes)	0	0.2	0.3	0.3	22.9	21.1	16.9	1.3
Bladder	0	0	0	0	19	18.4	16.9	5.4
Skin	20.8	25.4	28.3	20.5	26.2	18.9	21	31.2
Bone marrow	2.5	7.7	8.6	5.6	10.8	8.4	7.9	10.6

Table 3 Effective doses (mSv) as measured by LiF–TLD and as calculated using the $CTDI_w$. Effective doses standardized for 100 mAs for male and female subjects, and the dose-length product (DLP)

(mSv)	Neck	Chest			Abdomen			Spine
		Fast	Routine	HiRes	Fast	Routine	Angio	
Effective dose measured (male)	2.8	11.3	11.9	7.5	16.1	13.6	12.4	10.5
Effective dose calculated (male)	3.3	9.1	10.7	6.4	13.6	10.3	9.6	9.3
Effective dose (100 mAs; male)	2.8	9.9	9.4	10.8	9.8	10.5	12.4	8.1
Effective dose measured (female)	2.8	12.2	12.9	7.8	15.7	13.1	12.7	12.0
Effective dose calculated (female)	3.6	12.0	14.2	8.5	18.9	14.3	13.2	12.9
Effective dose (100 mAs; female)	2.8	10.2	10.8	11.1	9.5	10.0	12.7	9.2
DLP (mGy×cm)	171	298	364	173	531	341	244	449

Results

For standard MSCT of the chest with 5-mm slice collimation (Fast protocol), organs within the range of the primary beam revealed radiation doses from 19.5 mGy (liver) to 28.9 mGy (esophagus; Table 2). Organs outside this area, including the gonads, did not show radiation doses higher than 0.5 mGy. The effective dose applied by this routine MSCT protocol of the chest summed up to 12.2 mSv (females) and 11.3 mSv (males; Table 3).The dose distribution within the area of the primary beam was uniform including the surface skin dose (28.3 mGy).

In standard MSCT of the abdomen (5-mm slice collimation, Fast protocol), doses of organs within the primary beam were found to be within a range of 19.0 mGy (bladder) and 24.9 mGy (stomach). The surface dose in the area of the primary beam was 26.2 mGy. Table 2 demonstrates the distribution of relatively uniform organ doses throughout the abdomen. The effective dose added up to 15.7 mSv (females) and 16.1 mSv (males), respectively (Table 3).

For the Neck protocol, local organ doses ranged from 11.6 (thyroid) to 25.7 mGy (esophagus) in the area of the primary beam. Surface dose was 20.8 mGy. The effective dose was 2.8 mSv both for male and female subjects.

In the MSCT of the lumbar spine, colon, liver, and stomach revealed comparable doses of around 30 mGy. Surface dose was 31.2 mGy. Organs not exposed to the primary beam showed doses between 1.3 mGy (testes) and 8.7 mGy (ovaries). The effective dose was 10.5 mSv (males), and 12 mSv (females), respectively.

Only the Chest-MSCT protocol “Routine” with a narrower slice collimation revealed a slightly higher radiation dose compared with the Fast protocol. All other protocols of the chest or the abdomen showed lower effective doses, mainly due to different tube current-time settings. For Chest MSCT with 2.5-mm slice collimation (Routine), effective doses were 11.9 mSv (males) and 12.9 mSv (female). For the HiRes protocol with 1-mm slice collimation these data were 7.5 mSv (males) and 7.8 mSv (females), respectively.

In abdominal MSCT, the Routine protocol (2.5-mm slice collimation) showed 13.6 mSv (males) and 13.1 mSv (females). The effective dose for the Angio protocol was only slightly less: 12.4 mSv (males) and 12.7 mSv (females).

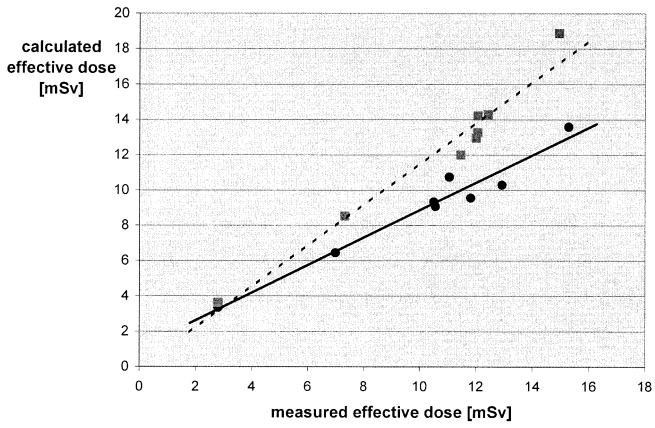

Fig. 1 Relation of effective doses for standard multi-slice CT (MSCT) scan protocols as measured by LiF–TLD vs calculated by CTDI. *Squares and dotted regression line* data for female subjects (y=1.163x-0.148; r=0.982); *circles and solid regression line* data for male subjects (y=0.7801x+1.0547; r=0.977)

The calculation of the effective dose on the basis of the weighted effective CTDI ($CTDI_{w,eff}$) underestimated the measured data mainly for male subjects. The calculation is relatively accurate for the chest protocols, whereas for the abdominal protocols the underestimation becomes more pronounced. Only for the Neck protocol, the calculated dose exceeded the measured data by 19%.

For female subjects, the calculation generally overestimated measured data. The calculated effective doses were 5% (Chest Fast protocol) to 30% (Neck protocol) higher than as measured by LiF–TLD (Table 3).

On direct comparison, a high degree of correlation between measured and calculated dose values was found (Fig. 1). The correlation coefficient was r=0.982 for "female" and r=0.977 for "male" data.

In order to be directly comparable to other protocols or CT scanners, different milliampere values need to be standardized to 100 mAs. This can simply be performed by dividing or multiplying effective doses accordingly. Table 3 displays these standardized effective doses. It becomes evident that with decreasing slice collimation despite an increase in pitch, the effective dose increases. In general, effective dose in abdominal CT is higher than in chest CT at comparable slice thicknesses.

Data for the calculated dose-length product are given in Table 3. Depending both on the scan length as well as on the CTDI, the DLP varies from 171 mGy×cm for the Neck protocol to 531 mGy×cm for the Abdomen Fast protocol.

Discussion

Computed tomography has been pushed to new borders by the development of multiple parallel detectors in order to improve either spatial or temporal resolution [1]. Different systems have been presented with up to 16 detector rows that acquire data during one tube rotation [14, 15]. As CT already leads to a relatively high radiation exposure disproportionate to its frequency of use, and the number of CT examinations will increase further, the objective of the present study was to provide data for further discussion on the aspect of radiation exposure of the patient undergoing multi-slice CT [6, 16].

In the present study, a CT system with four detector rows of different maximal width ("adaptive array detector") was used to assess radiation dose applied in several single-phase standard MSCT protocols implemented by the manufacturer for the neck, chest, abdomen, and lumbar spine. Effective doses vary between 2.8 and 16.1 mSv depending not only on the site of examination, but also on several technical factors such as tube current, tube potential, slice thickness, and pitch factor.

A particular problem of MSCT is the width of the fan beam in z-axis direction. As four or more detector chambers have to be exposed, a broader X-ray beam is used compared with the fan beam in single-slice CT. In order to avoid penumbral effects in the outer portions of the detector array, the primary collimation must be made wider than necessary to expose only the detector array [17]. Overbeaming is a characteristic of MSCT which reduces the portion of the beam that is captured by the detector array (beam efficiency). This is demonstrated by the normalized CTDI values derived in Table 3 which increase by up to 33% (female, abdominal protocols) when collimation is reduced from 4×5 to 4×1 mm. In other types of MSCT scanners, overbeaming may even be larger and can account for dose increases of up to 100% [17].

The geometric efficiency of multiple detectors added in z-axis direction is limited due to the interspacing strips and the reduced sensitivity at the edges of the row (shadow artifact) [13]. Previous work shows that a 30% dose increase may be expected due to this technical detail [17, 18]; however, with the advent of broader fan beams or the development of cone-beam techniques, this shortcoming may not be as relevant at present. It is noteworthy that in cases of an increased width of a fan or even a cone-beam scatter, radiation increases as well thus possibly degrading image quality.

Another effect may play a role in defining radiation exposure. Interpolation algorithms in spiral CT need data from areas above and below the actual volume or slice to be reconstructed [14, 15, 19]. Thus, at the beginning and the end of a scanned volume, the tube-detector system exposes areas that are not part of the area medically in question ("overscan"); therefore, a difference results between intended scan length of the area in question and the actual total table feed during exposure (Table 1). In case of a primary slice thickness of 5 mm, an overscan length of 40 mm is seen. Due to reduced slice thickness, the vol-

ume exposed but not reconstructed decreases to 12 mm; however, put into relation, the overscan volume necessary to reconstruct images increased from eight times the slice thickness (5 mm), ten times (2.5 mm), to even 12 times the primary slice thickness (MSCT, 1 mm).

It is well known from single-slice CT that a 50% increase in pitch leads to a dose reduction of approximately 30% [20, 21]. With our MSCT scanner, however, the software increased the tube current automatically by the same amount as that by which the pitch was increased. In order to counteract a possible degradation in image quality by an increased pitch, the Volume Zoom software was programmed to keep slice profile width, noise, and radiation exposure constant by automatic adaptation [13]. This is a characteristic of all MSCT scanners which make use of the so-called z-filtration [22]; thus, for the scanner used in this study, increasing the pitch factor only affects the speed of data acquisition, but no longer patient dose. Scanners which make use of a two-point z-interpolation (as in SSCT), however, behave differently.

Dose calculations using tabulated conversion coefficients are a convenient way to quickly estimate organ and effective doses. In this study, the dose calculations based on the weighted CTDI displayed at the console differed from the measured data by up to 30%. One explanation for the discrepancy observed in this study may be caused by differences in size and composition between the Alderson-Rando phantom and conditions considered for mathematical phantoms ("ADAM" and "EVA"). On the basis of tabulated conversion coefficients calculations of the effective dose can be performed [23]. Furthermore, the reliability of measurements with thermoluminescent dosimeters is limited and may be as low as ±3% but may reach up to 10% [24]. To minimize this effect and due to the relatively high detection threshold of LiF–TLD, we performed each protocol four times and divided the resulting data by four. In this study, discrepancies between calculations and TLD measurements of the effective dose of males was pronounced with a tendency to underestimation. An explanation may be that TLD located at the male gonads (testes) were exposed by the primary beam, whereas the conversion factors used for our calculational methods imply that male gonads are exposed by scatter radiation only [12, 13].

In general, calculated effective doses on the basis of the weighted CTDI show an excellent correlation to measured data [25, 26]. As the advantage of CTDI-based calculations lie in the ease of performance and the possibility to consider accurately the exact examination parameters, different computer software programs have been created to allow for dose calculations of individual examinations [27].

Compared with published data on radiation exposure by standard examination settings in single-slice spiral CT (SSCT), multi-slice CT seems to have considerably higher doses. The SSCT examinations lead to effective doses of approximately 5–20 mSv [6, 28, 29, 30]. As our study only comprises one complete scan from the dome of the diaphragm to the perineum, even higher doses may be reached in MSCT, when two or three hepatic perfusion phases are examined or when delayed scans are necessary, e.g., to investigate the suprarenal glands or the urogenital tract. Obviously, in chest CT low-dose or dose-reduced protocols are often used and the mean effective dose in the general population examined for medical reasons may be lower. Efforts to reduce radiation dose will be made as first reports hint at relevant dose reduction potentials even for new diagnostic fields [5, 31].

Limits of this study include that data apply only to an MSCT scanner with adaptive array detector system. The inner detector arrays are smaller than the ones at the outer zone. No overlapping protocols were analyzed. The extent to which differences between manufacturers, either in technical solutions or software-related aspects, influence radiation dose remains to be elucidated in further studies. Furthermore, Alderson-Rando phantoms can only imitate human tissue and its quality with respect to X-ray absorption; however, the individual radiation exposure of organs, and therefore the individual effective dose, cannot be determined in vivo.

In conclusion, radiation exposure in standard multislice CT protocols of the neck, chest, abdomen, and lumbar spine ranges from 3 to 15 mSv. Radiation dose increases with decreasing slice thickness. Several technical details and physical characteristics of multi-slice scanners may be responsible for these results. Considering published data, an increase in dose compared with single-slice CT is to be expected. In view of expanding indications and numbers of CT examinations, further efforts are needed to reduce dose and therefore patient exposure.

Acknowledgement The authors are indebted to H.-D. Nagel, Philips Medical Systems, Hamburg, for valuable hints and thorough discussion of the topic.

References

1. Fuchs T, Kachelriess M, Kalender WA (2000) Technical advances in multi-slice spiral CT. Eur J Radiol 36:69–73
2. Ghaye B, Szapiro D, Willems V, Dondelinger RF (2000) Combined CT venography of the lower limbs and spiral CT angiography of pulmonary arteries in acute pulmonary embolism: preliminary results of a prospective study. JBR-BTR 83:271–278
3. Hara AK, Johnson CD, MacCarty RL, Welch TJ, McCollough CH, Harmsen WS (2001) CT colonography: single- versus multi-detector row imaging. Radiology 219:461–465

4. Knez A, Becker CR, Leber A, Ohnesorge B, Becker A, White C, Haberl R, Reiser MF, Steinbeck G (2001) Usefulness of multislice spiral computed tomography angiography for determination of coronary artery stenoses. Am J Cardiol 88:1191–1194
5. Ohnesorge B, Flohr T, Becker C, Kopp AF, Schoepf UJ, Baum U, Knez A, Klingenbeck-Regn K, Reiser MF (2000) Cardiac imaging by means of electrocardiographically gated multisection spiral CT: initial experience. Radiology 217:564–571
6. Kaul A, Bauer B, Bernhardt J, Nosske D, Veit R (1997) Effective doses to members of the public from the diagnostic application of ionizing radiation in Germany. Eur Radiol 7:1127–1132
7. Cohnen M, Poll L, Puttmann C, Ewen K, Modder U (2001) Radiation exposure in multi-slice CT of the heart. Fortschr Rontgenstr 173:295–299
8. ICRP International Commission on Radiological Protection (1975) Reference man: anatomic, physiological and metabolic characteristics. ICRP, publication no. 23. Pergamon, Oxford
9. Fung KK, Gilboy WB (2001) The effect of beam tube potential variation on gonad dose to patients during chest radiography investigated using high sensitivity LiF:Mg,Cu,P thermoluminescent dosemeters. Br J Radiol 74:358–367
10. ICRP International Commission on Radiological Protection (1991) 1990 recommendation of the International Commission on Radiological Protection. ICRP publication no. 60. Pergamon, Oxford
11. McCollough CH, Schueler BA (2000) Calculation of effective dose. Med Phys 27:828–837
12. Hidajat N, Vogl T, Schroder RJ, Felix R (1996) Berechnete Organdosen und effektive Dosis für die computertomographische Untersuchung des Thorax und des Abdomens: sind diese Dosen realistisch? Fortschr Rontgenstr 164:382–387
13. Nagel H-D, Galanski M, Hidajat N, Maier W, Schmidt T (2000) Radiation exposure in computed tomography: fundamentals, influencing parameters, dose assessment, optimization, scanner data, terminology. COCIR, Frankfurt
14. Fuchs TO, Kachelriess M, Kalender WA (2000) System performance of multislice spiral computed tomography. IEEE Eng Med Biol Mag 19:63–70
15. Ohnesorge B, Flohr T, Schaller S, Klingenbeck-Regn K, Becker C, Schopf UJ, Bruning R, Reiser MF (1999) Technische Grundlagen und Anwendungen der Mehrschicht-CT. Radiologe 39:923–931
16. Wessling J, Fischbach R, Ludwig K, Juergens KU, Schaller S, Fallenberg EM, Lenzen H, Heindel W (2001) Mehrschicht-Spiral-CT des Abdomens bei onkologischen Patienten: Einfluss von Tischvorschub und Detektorkonfiguration auf Bildqualität und Strahlenexposition. Fortschr Rontgenstr 173:373–378
17. McCollough CH, Zink FE (1999) Performance evaluation of a multi-slice CT system. Med Phys 26:2223–2230
18. Klingenbeck-Regn K, Schaller S, Flohr T, Ohnesorge B, Kopp AF, Baum U (1999) Subsecond multi-slice computed tomography: basics and applications. Eur J Radiol 31:110–124
19. Taguchi K, Aradate H (1998) Algorithm for image reconstruction in multi-slice helical CT. Med Phys 25:550–561
20. Cohnen M, Fischer H, Hamacher J, Lins E, Kotter R, Modder U (2000) CT of the head by use of reduced current and kilovoltage: relationship between image quality and dose reduction. Am J Neuroradiol 21:1654–1660
21. Hidajat N, Maurer J, Schroder RJ, Wolf M, Vogl T, Felix R (1999) Radiation exposure in spiral computed tomography. Dose distribution and dose reduction. Invest Radiol 34:51–57
22. Takahashi M, Maguire WM, Ashtari M, Khan A, Papp Z, Alberico R, Campbell W, Eacobacci T, Herman PG (1998) Low-dose spiral computed tomography of the thorax: comparison with the standard-dose technique. Invest Radiol 33:68–73
23. Zankl M, Panzer W, Drexler G (1995) The calculation of dose from external photon exposures using reference human phantoms and Monte Carlo methods. VI. Organ doses from computed tomographic examinations. GSF-Forschungszentrum, Neuherberg
24. Paul JM, Khan FR (1975) Dosimetric reliability of thermoluminescent phosphors (TLD-too). J Radiol Electrol Med Nucl 56:779–783
25. Geleijns J, Van Unnik JG, Zoetelief J, Zweers D, Broerse JJ (1994) Comparison of two methods for assessing patient dose from computed tomography. Br J Radiol 67:360–365
26. Hidajat N, Maurer J, Schroder RJ, Nunnemann A, Wolf M, Pauli K, Felix R (1999) Relationships between physical dose quantities and patient dose in CT. Br J Radiol 72:556–561
27. Kalender WA, Schmidt B, Zankl M, Schmidt M (1999) A PC program for estimating organ dose and effective dose values in computed tomography. Eur Radiol 9:555–562
28. Hidajat N, Wolf M, Nunnemann A, Liersch P, Gebauer B, Teichgraber U, Schroder RJ, Felix R (2001) Survey of conventional and spiral CT doses. Radiology 218:395–401
29. Scheck RJ, Coppenrath EM, Kellner MW, Lehmann KJ, Rock C, Rieger J, Rothmeier L, Schweden F, Bauml AA, Hahn K (1998) Radiation dose and image quality in spiral computed tomography: multicentre evaluation at six institutions. Br J Radiol 71:734–744
30. Van Unnik JG, Broerse JJ, Geleijns J, Jansen JT, Zoetelief J, Zweers D (1997) Survey of CT techniques and absorbed dose in various Dutch hospitals. Br J Radiol 70:367–371
31. Kachelriess M, Watzke O, Kalender WA (2001) Generalized multi-dimensional adaptive filtering for conventional and spiral single-slice, multi-slice, and cone-beam CT. Med Phys 28:475–490